Published in final edited form as:
Neuron. 2014 May 7; 82(3): 659–669. doi:10.1016/j.neuron.2014.03.011.

SNX27 regulation of GIRK channels in VTA dopamine neurons attenuates *in vivo* cocaine response

Michaelanne B. Munoz[1,2] and **Paul A. Slesinger**[1,2,3,§]

[1]Peptide Biology Laboratories, The Salk Institute for Biological Studies, La Jolla, CA 92037

[2]Graduate Program in Biology, University of California, San Diego, La Jolla, CA 92093

[3]Dept. of Neuroscience, Icahn School of Medicine at Mount Sinai, New York, NY

Abstract

The subcellular pathways that regulate G protein-gated inwardly rectifying potassium (GIRK or Kir3) channels are important for controlling the excitability of neurons. Sorting nexin 27 (SNX27) is a PDZ-containing protein known to bind GIRK2c/3 channels but its function in vivo is poorly understood. Here, we investigated the role of SNX27 in regulating GIRK currents in dopamine (DA) neurons of the ventral tegmental area (VTA). Mice lacking SNX27 in DA neurons exhibited reduced $GABA_BR$-activated GIRK currents but had normal I_h currents and dopamine D2R-activated GIRK currents. Expression of GIRK2a, a SNX27-insensitive splice-variant, restored $GABA_BR$-activated GIRK currents in SNX27-deficient DA neurons. Remarkably, mice with significantly reduced $GABA_BR$-activated GIRK currents in only DA neurons were hypersensitive to cocaine, and could be restored to a normal locomotor response with GIRK2a expression. These results identify a novel pathway for regulating excitability of VTA DA neurons, highlighting SNX27 as a promising target for treating addiction.

Introduction

Dopamine (DA) is an important neuromodulator of incentive salience, encoding both rewarding and aversive responses *in vivo*. Dysfunction in DA signaling has been implicated in a variety of psychiatric disorders including drug addiction, anxiety, and schizophrenia (Schultz, 2007). Dopaminergic neuronal cell bodies are concentrated in two main nuclei in the midbrain, the ventral tegmental area (VTA) and the substantia nigra (SN). The actions of addictive drugs converge on VTA DA neurons, where they increase DA neuron activity and the level of DA released in projection areas (Lüscher and Malenka, 2011). Exposure to addictive drugs, even acutely, produces persistent adaptations in excitatory and inhibitory pathways within the mesolimbic dopamine circuit, establishing the building blocks

[§]Correspondence: Paul A. Slesinger, Dept. of Neuroscience, Icahn School of Medicine at Mount Sinai, One Gustave L. Levy Place, New York, NY 10029. paul.slesinger@mssm.edu.

underlying addiction (Arora et al., 2011; Liu et al., 2005; Mameli et al., 2011; Padgett et al., 2012; Saal et al., 2003; Ungless et al., 2001).

Inhibitory pathways primarily involve GABA, which activates fast $GABA_A$-type receptors and slower G protein-coupled $GABA_B$ receptors. Repeated exposure to cocaine reduces the amplitude of fast GABA-evoked IPSCs, promoting LTP induction (Liu et al., 2005), and genetic manipulation of $GABA_A$ receptors in DA neurons enhances reward learning and morphine response (Parker et al., 2011). Activation of $GABA_B$ receptors inhibits DA neuronal firing activity (Johnson and North, 1992; Seutin et al., 1994), reduces dopamine release (Klitenick et al., 1992), and provides a mechanism for opposing the reinforcing effects of drugs of abuse (Kalivas and Stewart, 1991). Previous studies have implicated $GABA_B$ receptors coupled to G protein-gated inwardly rectifying potassium (GIRK or Kir3) channels in the response to drugs of abuse (Cruz et al., 2004; Labouèbe et al., 2007; Luscher et al., 1997; Morgan et al., 2003; Padgett et al., 2012), with both $GABA_B$ receptors and GIRK channels emerging as an important therapeutic target for neurological disorders (Lujan et al., 2013; Lüscher and Slesinger, 2010; Tyacke et al., 2010).

In contrast to the plethora of cytoplasmic and membrane proteins known to regulate trafficking of excitatory glutamate receptors (Kim and Sheng, 2004; Sumioka, 2013), relatively few subcellular pathways have been described for regulating GIRK channel expression. One pathway involves a change in phosphorylation of GIRK2 channels in the hippocampus, whereby dephosphorylation of a serine residue preceding an internalization motif promotes channel recycling (Chung et al., 2009). In addition, GIRK3 channels contain a lysosomal targeting motif that can target GIRK3-containing channels for lysosomal degradation (Ma et al., 2002). Another regulatory pathway involves association of an endosomal sorting nexin 27 (SNX27) protein with GIRK channels (Balana et al., 2011; Lunn et al., 2007). Thus far, SNX27 is the only cytoplasmic protein known to selectively bind GIRK channels (Balana et al., 2011; Lunn et al., 2007).

SNX27 belongs to a family of endosomal sorting proteins, defined by the presence of a phox-homology (PX) domain, which binds phosphatidylinositol-3-monophosphate (PI3P) in the early endosome (EE) (Cullen and Korswagen, 2011). Of the ~33 sorting nexins described to date, SNX27 is unique because it is the only sorting nexin that contains a PDZ (post synaptic density (PSD)-95, discs large, zona occludens) domain. We showed previously that the PDZ domain of SNX27 associates directly with the C-terminal PDZ binding motif in GIRK2c/GIRK3 subunits (Balana et al., 2011; Lunn et al., 2007). In heterologous expression systems and hippocampal neurons, overexpression of SNX27 reduces the amplitude of $GABA_B$R-activated GIRK currents (Balana et al., 2011; Lunn et al., 2007) and in rodent neocortex, RNA expression is regulated by psychostimulant exposure (Kajii et al., 2003). SNX27 also regulates other signaling proteins, including glutamate receptors (Wang et al., 2013), 5-HT receptors (Joubert et al., 2004), multidrug resistance-associated protein 4 (Hayashi et al., 2012) and β2 adrenergic receptors (Lauffer et al., 2010). For β2 adrenergic receptors, knockdown of SNX27 by RNAi in cultured aortic smooth muscle cells decreases forward trafficking of β2 adrenergic receptors, leading to reduced adrenergic signaling (Lauffer et al., 2010). How endogenously expressed SNX27 regulates GIRK channel expression *in vivo* remains an important but unanswered question.

Mice with a complete SNX27 null mutation, however, exhibit severe developmental defects and die postnatally (Cai et al., 2011), precluding assessment of SNX27 on GIRK function *in vivo*. Heterozygote $SNX27^{+/-}$ mice, on the other hand, appear to have normal neurodevelopment but exhibit defects in excitatory neurotransmission in the hippocampus, due to reduced levels of AMPA and NMDA receptors (Wang et al., 2013).

To investigate the function of natively expressed SNX27 *in vivo* and overcome the obstacle of severe developmental defects, we created a mouse mutant that lacks SNX27 protein in only DA neurons. VTA DA neurons exclusively express GIRK2c and GIRK3 subunits, which contain the PDZ-binding motif required for interacting with SNX27 (Cruz et al., 2004; Lunn et al., 2007). We hypothesized that SNX27 will be required for GIRK function in the VTA DA neurons. We discovered that SNX27 is an essential regulator of $GABA_BR$-activated GIRK signaling in VTA DA neurons and helps mitigate the stimulatory effects of cocaine, implicating SNX27 as a promising therapeutic target for treating addiction.

Results

SNX27 controls amplitude of $GABA_BR$-activated GIRK currents in VTA DA neurons

Postnatal mice containing a null mutation in the SNX27 gene exhibit severe developmental defects and die before weaning (Cai et al., 2011), indicating that SNX27 is involved in multiple signaling pathways in the mouse. Indeed, SNX27 is expressed in a variety of cell types, including brain, heart, kidney and lung (Kajii et al., 2003). To avoid lethality, we created a conditional knockout of SNX27 in mice that targeted only DA neurons (Figure 1A – see Methods for details). This was accomplished by crossing a pre-conditional floxed *Snx27* line ($Snx27^{fl/fl}$) with a DAT-$Cre^{+/-}$ line, where Cre recombinase expression is under the control of the dopamine transporter gene (DAT or Slc6j) (Zhuang et al., 2005) (Figure 1A). As expected, immunostaining for SNX27 protein revealed a loss of SNX27 protein expression in midbrain TH-positive neurons of DAT-$Cre^{+/-}$ × $Snx27^{fl/fl}$ mice, which we refer to as $SNX27_{DA}$ KO mice (Figure 1A–C). Importantly, $SNX27_{DA}$ KO mice were viable, bred normally and lived into adulthood. Moreover, the number of TH positive neurons in the VTA/SN did not appear to differ from control mice (Figure 1D). We next examined the viability of VTA DA neurons using whole-cell patch clamp electrophysiology in 3–4 week old mice. Dopamine neurons were identified by presence of an I_h current, slow firing frequency and by Cre-dependent expression of fluorescent proteins when available (Cruz et al., 2004; Labouèbe et al., 2007; Padgett et al., 2012). Other types of VTA DA neurons exist, which lack I_h and project to mPFC, but these neurons do not possess D2R-activated GIRK currents (Lammel et al., 2008). VTA DA neurons in acutely prepared horizontal midbrain slices from $SNX27_{DA}$ KO mice had input resistances, resting membrane potentials and cell sizes indistinguishable from those in wild-type neurons (Figure 1E & Supplemental Table 1). Similarly, loss of SNX27 in DA neurons did not significantly change the amplitude of I_h current (Figure 1F). Taken together, these results suggest that there were no gross changes in function of DA neurons lacking SNX27.

VTA DA neurons express a robust $GABA_BR$-activated GIRK current (I_{Ba}clofen) (Arora et al., 2011; Cruz et al., 2004; Padgett et al., 2012). In pre-conditional $Snx27^{fl/fl}$ littermates (referred to as wild-type; WT) and DAT-$Cre^{+/-}$ controls, bath application of a saturating

concentration of the $GABA_BR$ agonist baclofen (300μM) activated a large outward $GABA_BR$-activated GIRK current (203.6 ± 21.3 pA, n=17 for WT; 246.1 ± 24.6 pA, n=18 for Dat-$Cre^{+/-}$); I_{Ba}clofen was completely suppressed by the selective K_{ir} channel inhibitor Ba^{2+} (Cruz et al., 2004) (Figure 2A). In DA neurons of $SNX27_{DA}$ KO mice the $GABA_BR$-activated GIRK current was ~60% smaller; 74.7 ± 9.2 pA, n=18 (**p<0.01, one-way ANOVA with Bonferroni post hoc test) (Figure 2B). Dopamine D2R-activated GIRK currents revealed with bath application of quinpirole (30 μM) were similar in size for $SNX27_{DA}$ KO and control mice (Figure 2C,D), 47.0 ± 9.1 pA, n=13 for WT; 54.3 ± 14.2 pA, n= 8 for Dat-$Cre^{+/-}$ and 34.9 ± 9.1 pA, n= 14 for $SNX27_{DA}$ KO, $p > 0.05$). To investigate the potential effect of SNX27 KO on fast $GABA_A$ currents, we measured the spontaneous fIPSCs in VTA DA neurons of $SNX27_{DA}$ KO mice (Bocklisch et al., 2013). Neither the mean amplitude nor instantaneous frequency appeared to be different in the $SNX27_{DA}$ KO mice, as compared to Dat-$Cre^{+/-}$ mice (see Supplemental Table 1). Thus, selective disruption of SNX27 expression in VTA DA neurons appears to preferentially affect $GABA_BR$-activated GIRK currents.

VTA DA neurons receive inhibitory inputs from local and projection GABA neurons (Floresco et al., 2003; Jhou et al., 2009; Padgett et al., 2012). Because activation of $GABA_BR$-GIRK currents in VTA is sufficient to inhibit phasic firing of DA neurons (Seutin et al., 1994), we wondered whether the reduced $GABA_BR$-activated GIRK current would be sufficient to alter inhibitory control of neuronal activity. We constructed input-output curves for induced firing measured in current-clamp mode for wild-type and $SNX27_{DA}$ KO DA neurons (Figure 3). Remarkably, a saturating concentration of baclofen (300 μM) failed to inhibit firing induced over a range of current injections in DA neurons of $SNX27_{DA}$ KO mice, in contrast to wild-type controls (Figure 3A–D).

SNX27 controls surface expression of GIRK channels

We next asked whether the reduction in $GABA_BR$-activated GIRK currents could be explained by a decrease in surface expression of $GABA_B$ receptors or alternatively, a decrease in GIRK channel expression (Cruz et al., 2004; Padgett et al., 2012; Terunuma et al., 2010). To investigate a change in surface expression of GIRK channels, we examined the effect of intracellular GTPγS, a non-hydrolyzable form of GTP that bypasses GPCR activation and constitutively activates GIRK channels via a Gβγ-dependent mechanism (Logothetis et al., 1987). If the absence of SNX27 protein affected the function of only $GABA_B$ receptors, then GTPγS-stimulated currents would be expected to be similar in size to those of control neurons. In control neurons (WT and DAT-$Cre^{+/-}$), inclusion of 100 μM GTPγS in the intracellular solution led to slow activation of a large outward potassium current, which was subsequently inhibited with extracellular Ba^{2+}, indicating activation of GIRK channels (Figure 4A). In VTA DA neurons of $SNX27_{DA}$ KO mice, however, the GTPγS-induced Ba^{2+}-sensitive currents were significantly reduced (Figure 4B). On average, the GTPγS-stimulated currents were ~75% smaller in $SNX27_{DA}$ KO mice (161.0 ± 21.7, n=13 for WT; 117.9 ± 7.5, n=11 for Dat-$Cre^{+/-}$; 33.2 ± 5.7, n=8 for $SNX27_{DA}$ KO, $p < 0.05$), similar to the reduction in $I_{Baclofen}$. These results suggest SNX27 is important for regulating surface expression of GIRK channels coupled to $GABA_B$ receptors in DA neurons.

SNX27 control of GIRK expression requires PDZ domain interaction

Expression of SNX27 is known to be important for mouse development (Cai et al., 2011). We therefore wanted to rule out the possibility that loss of SNX27 in DA neurons during neurodevelopment did not indirectly affect the expression of GIRK channels. To address this possibility, we expressed SNX27 selectively in DA neurons of 4-week-old $SNX27_{DA}$ KO mice and then measured the amplitude of $GABA_BR$-activated GIRK currents in DA neurons after 2–3 weeks. Both splice variants, SNX27a and SNX27b, are developmentally regulated (Kajii et al., 2003). Because SNX27b is sensitive to psychostimulants (Kajii et al., 2003), we engineered *Snx27b* into an adeno-associated virus (AAV; serotype 5), with a double floxed inverted (DIO) *Snx27b*-ires-GFP sequence under the control of EF1a promoter (Tsai et al., 2009) (Figure 5A). In the DAT-$Cre^{+/-}$ line, injection of AAV DIO *Snx27b*-ires-GFP limits expression of SNX27b to neurons containing Cre recombinase, which is expressed in DAT+ neurons. For control, we studied the effect of injecting AAV DIO-eYFP, a similar virus that lacks SNX27b. In $SNX27_{DA}$ KO mice with either AAV DIO *Snx27b*-ires-GFP or AAV DIO-eYFP stereotaxically injected into the VTA, we observed GFP/YFP expression in midbrain sections after 12–20 days (Figure 5A). We then recorded baclofen-induced $GABA_BR$-activated GIRK currents ($I_{Baclofen}$) in GFP/YFP positive neurons (Fig. 5A,B). Similar to uninjected $SNX27_{DA}$ KO mice (Figure 2B), $I_{Baclofen}$ was reduced by approximately 70% (66.2 ± 14.1 pA, n=6) for mice injected with AAV DIO-eYFP (Figure 5B). By contrast, $I_{Baclofen}$ was larger in DA neurons of $SNX27_{DA}$ KO mice injected with AAV DIO-*Snx27b*-ires-GFP (236.9 ± 47.7 pA, n=6) (Figure 5B), similar to wild-type $I_{Baclofen}$ (Figure 2B). Moreover, $GABA_BR$-dependent inhibition of neuronal firing in DA neurons of $SNX27_{DA}$ KO mice acutely expressing SNX27b was indistinguishable from wild-type neurons and significantly greater than in $SNX27_{DA}$ KO mice expressing eYFP (Figure 5C,D). Taken together, these results demonstrate that restoring SNX27 expression in DA neurons was sufficient to rescue $GABA_BR$-activated GIRK currents and inhibitory control of firing, making a developmental defect as the cause of reduced $GABA_BR$-activated GIRK currents highly unlikely.

Both SNX27a and SNX27b contain a single PDZ domain that is essential for its regulation of GIRK channels (Lunn et al., 2007). This PDZ interaction is mediated by a PDZ binding motif, ‘E(N/S)ESKV’, which is present on the C-terminus of GIRK2c and GIRK3 channels (Balana et al., 2011; Lunn et al., 2007). We hypothesized that the reduced $GABA_BR$-activated GIRK currents in $SNX27_{DA}$ KO mice occurred because endogenous PDZ-interacting GIRK2c and GIRK3 subunits required SNX27 for expression (Cruz et al., 2004). To investigate the role of the PDZ binding motif in GIRK2, we constructed an AAV to express the splice variant GIRK2a, which lacks a PDZ binding motif and does not associate with SNX27 (Balana et al., 2011; Lunn et al., 2007). In addition, GIRK2a is capable of forming homotetramers and thus functional channels (Inanobe et al., 1999). $SNX27_{DA}$ KO mice were injected with AAV DIO-*Girk2a*-eYFP or AAV DIO-eYFP, as described above, and midbrain slices were prepared for whole-cell patch-clamp recordings (Figure 6A,B). As expected, mean $I_{Baclofen}$ currents were smaller in $SNX27_{DA}$ KO mice injected with AAV DIO-eYFP, 80.2 ± 16.9 pA, n=8 (Figure 6B). Remarkably, $I_{Baclofen}$ significantly increased by 3-fold in DA neurons of $SNX27_{DA}$ KO mice injected with AAV DIO GIRK2a-eYFP, 240.9 ± 50.8 pA, n=8 (Figure 6B). Moreover, $GABA_BR$-dependent inhibition of action

potential firing was restored to that observed in wild-type neurons (Figure 6C,D). Taken together, these experiments suggest that SNX27 is required for forward trafficking and/or maintenance of GIRK2c/GIRK3 channels on the plasma membrane in DA neurons and is important for controlling the excitability of DA neurons.

Enhanced cocaine response in $SNX27_{DA}$ KO mice

The reduction of $GABA_BR$-activated GIRK currents in VTA DA neurons of $SNX27_{DA}$ KO mice afforded us with a unique opportunity to explore the behavioral effects of the subtle change in electrical properties of VTA DA neurons. In previous experiments with $GABA_B$-R agonists or antagonists, it was not possible to selectively target $GABA_BR$-activated GIRKs in DA neurons (Frankowska et al., 2009; Kalivas and Stewart, 1991). Previous studies have shown that firing of VTA DA neurons is critically involved in reward processing and the response to drugs of abuse (Kalivas and Stewart, 1991; Parker et al., 2011; Schultz, 2007; Tsai et al., 2009). We therefore investigated whether the reduced $GABA_BR$-activated GIRK currents in VTA DA neurons of $SNX27_{DA}$ KO mice would affect the response to cocaine. Interestingly, basal locomotor activity of $SNX27_{DA}$ KO mice was ~40% higher upon initial exposure to a novel open field environment, as compared to wild-type or DAT-$Cre^{+/-}$ control mice (Figure 7A). However, $SNX27_{DA}$ KO mice occupied the center of the chamber for the same amount of time as controls (Figure 7B), ruling out altered thigmotaxis (wall-hugging) or anxiety levels as possible explanations for enhanced activity levels.

Psychostimulants increase locomotion through stimulation of VTA DA neurons (Vanderschuren and Kalivas, 2000). To investigate the response of $SNX27_{DA}$ KO mice to psychostimulants, we injected cocaine (20 mg/kg; i.p.) and immediately measured the total distance traveled over 30 minutes in an activity chamber. In WT and Dat-$Cre^{+/-}$ controls, cocaine increased locomotor activity by ~3-fold, 3.2 ± 0.5 fold for WT, n=6; 2.7 ± 0.4 fold for DAT-$Cre^{+/-}$, n=16 (Figure 7C,D). By contrast, a single injection of cocaine increased locomotor activity by 8.0 ± 1.7 fold (n=14) in $SNX27_{DA}$ KO mice (Figure 7C,D), suggesting that the reduced $GABA_BR$-activated GIRK currents contributed to the heightened response to cocaine. To determine if the change in $GABA_BR$-activated GIRK signaling alone was sufficient to alter the response to cocaine, we took advantage of the finding that $GABA_BR$-activated GIRK currents and $GABA_B$-dependent inhibition of firing were restored in $SNX27_{DA}$ KO mice injected with AAV DIO GIRK2a-eYFP (Figure 6B & Figure 8B). We next investigated the effect of cocaine in $SNX27_{DA}$ KO mice with AAV DIO GIRK2a-eYFP injected into VTA. Remarkably, the increase in locomotor activity produced in response to cocaine returned to control levels in $SNX27_{DA}$ KO mice expressing GIRK2a (Figure 8B,C). Reduction of the amplitude of fast GABA-evoked IPSCs can increase excitability DA neurons and enhance the locomotor response to morphine (Parker et al., 2011), but we did not observe a change in frequency or amplitude of sIPSCs in $SNX27_{DA}$ KO neurons. Thus, alterations in the amplitude of $GABA_BR$-activated GIRK currents in VTA DA neurons appears tightly correlated with the response to cocaine, implicating SNX27 as a potential therapeutic target for dopamine-dependent behavioral disorders such as addiction.

Discussion

Elucidating the subcellular pathways that regulate G protein-gated inwardly rectifying potassium (GIRK or Kir3) channels is important for understanding control of neural circuits in the brain. Here, we show for the first time that SNX27 plays a key role in regulating neuronal excitability of DA neurons, likely through control of GIRK channel trafficking. Loss of SNX27 leads to reduced $GABA_BR$-activated GIRK currents, which was sufficient to alter the stimulatory response to cocaine. Altered VTA inhibitory control has been implicated in a number of psychiatric disorders, including response to addictive drugs (Lüscher and Malenka, 2011), aversive stimuli (Jhou et al., 2009), and depression (Tye et al., 2012). Targeting inhibitory signaling may emerge as an alternative strategy for novel therapeutic interventions for treating addiction (Lujan et al., 2013).

What is the subcellular mechanism underlying reduced $GABA_BR$-activated GIRK currents in DA neurons lacking SNX27? One possibility is that SNX27 alters the maturation of DA neurons and subsequent GIRK expression, since SNX27 has been shown to be important during neurodevelopment (Cai et al., 2011; Kajii et al., 2003). This scenario seems unlikely since ectopic expression of SNX27 in DA neurons of $SNX27_{DA}$ KO mice completely restored $GABA_BR$-GIRK currents to wild-type levels. Furthermore, basic electrical properties and fast inhibitory synaptic inputs were unaltered in VTA DA neurons lacking SNX27. Another explanation is that loss of SNX27 affected other signaling proteins that indirectly altered GIRK expression. For example, SNX27 interacts with glutamate receptors (Cai et al., 2011; Wang et al., 2013), 5-HT receptors (Joubert et al., 2004) and β2 adrenergic receptors (Lauffer et al., 2010). However, expressing GIRK2a in VTA DA neurons restored $GABA_BR$-GIRK currents to wild-type levels, indicating that the essential proteins needed for $GABA_BR$-activated GIRK signaling are present once GIRK channels are expressed on the plasma membrane. The simplest explanation for the reduced $GABA_BR$-activated GIRK currents is that fewer GIRK channels traffic to the plasma membrane in the SNX27 KO mice. Thus, maximal activation of GIRK channels by intracellular GTPγS application, which bypasses GPCR activation, is lower in DA neurons lacking SNX27. Restoration of $GABA_BR$-activated GIRK currents with a GIRK2 variant (GIRK2a) lacking the PDZ binding motif needed to associate with the PDZ domain of SNX27 suggests that SNX27 is required for forward trafficking and/or maintenance of GIRK2c/3 subunits on the plasma membrane. This regulation may be restricted to PDZ-containing proteins since general endosomal trafficking appears to remain intact in the absence of SNX27 (Cullen and Korswagen, 2011).

Previous studies support a role for SNX27 in regulating forward trafficking of signaling proteins. In cultured aortic cardiac cells, RNAi knockdown of SNX27 lowered β2-adrenergic receptor expression on the plasma membrane (Lauffer et al., 2010; Temkin et al., 2011). Similarly, reduced levels of SNX27 protein in a heterozygote SNX27-deficient mice ($Snx27^{+/-}$) reduced forward trafficking of GluR1 and NR1 glutamate receptors in hippocampus (Wang et al., 2013). A more detailed analysis of β2-adrenergic receptor recycling revealed that sorting nexin 27 (SNX27) links β2-adrenergic receptors to the retromer tubule, which is important for recycling back to the plasma membrane (Temkin et al., 2011). In addition to the PDZ domain and PX domain, SNX27 contains a RA / FERM

domain that is proposed to bind Ras-like GTPase proteins (Balana et al., 2013; Ghai et al., 2011); perhaps the RA domain recruits additional binding partners to regulate interaction with the retromer complex and trafficking from the early endosome. Using a proteomics approach, Steinberg et al. (2013) discovered over 100 cell surface proteins that required a SNX27–retromer to prevent lysosomal degradation and maintain surface levels. It will be important to establish if the same retromer pathway exists for GIRK channels in SNX27-mediated recycling.

Remarkably, lack of SNX27 protein in VTA DA neurons appeared to have a greater effect on $GABA_BR$-activated GIRK currents than D2R-activated GIRK currents. Thus, D2R and $GABA_BR$ signaling complexes may be differentially regulated in DA neurons. $GABA_B$ receptors have been shown to form macromolecular complexes with muscarinic receptors (Boyer et al., 2009), extracellular calcium sensing receptor (Chang et al., 2007) and GIRK channels (Ciruela et al., 2010; Fowler et al., 2007; Labouèbe et al., 2007; Lujan et al., 2009; Zhou et al., 2012). It is unknown whether D2 receptors also form distinct complexes with GIRK channels in DA neurons. GPCRs can be distinctly regulated based on compartmentalization or access to regulatory elements (Gainetdinov et al., 2004). Another possibility is that D2R and $GABA_BR$ couple to different subunit compositions of GIRK channels. For example, D2 receptors may selectively activate GIRK2 homotetramers, while $GABA_B$ receptors may couple to GIRKc2-GIRK3 heteromultimers. Accordingly, SNX27 preferential association with GIRK2c/3 (Lunn et al., 2007) would selectively target $GABA_BR$-activated GIRK channels. In support of this idea, expression of GIRK2a in DA neurons lacking SNX27 led to slightly larger D2R-activated currents (54 ± 14 pA N=8 for Dat-$Cre^{+/-}$ and 71 ± 22 pA N=6 for GIRK2a in $SNX27_{DA}$ KO), though additional experiments are needed to substantiate this finding.

Curiously, overexpression of SNX27 in hippocampal neurons leads to smaller $GABA_BR$-activated GIRK currents (Balana et al., 2011), a seemingly unexpected finding in context of smaller $GABA_BR$-activated GIRK currents in VTA DA neurons lacking SNX27. Ectopic expression of SNX27 targets 5-HT4a serotonergic receptors (Joubert et al., 2004) and GIRK channels (Lunn et al., 2007) proteins to the early endosome, where it can affect the trafficking of proteins. One possibility is that high levels of SNX27 protein act as a negative regulator of forward trafficking (Lauffer et al., 2010). Previous studies have shown that abnormal levels of key endocytic proteins impair homeostasis of protein networks and disrupt activity. SNX9, for example, is able to form dimers, and therefore increased SNX9 expression has been suggested to act as a dominant negative, leading to similar defects in recycling as is observed following protein knockdown (Shin et al., 2007). Similarly, both overexpression and RNAi knockdown of SPIN90 decreased synaptic vesicle endocytosis (Kim et al., 2005). Recently, SNX27 was found to form a tripartite complex with β-Pix, which associated directly with SNX27, and indirectly with a G protein-coupled receptor kinase interacting protein (Git1) (Valdes et al., 2011). Both dimerization and multimeric protein complex formation offer intriguing mechanisms to regulate GIRK channel trafficking through altered SNX27 expression *in vivo* and remain an exciting area for future investigation.

In vivo exposure to cocaine or methamphetamine decreases $GABA_BR$-activated GIRK currents in VTA neurons (Arora et al., 2011; Padgett et al., 2012) and cortical neurons (Hearing et al., 2013), all appearing to result from reduced surface expression of GIRK channels. For VTA GABA neurons and PFC pyramidal neurons, a change in phosphorylation of the $GABA_B$ receptor may guide the change in $GABA_BR$-activated GIRK currents (Hearing et al., 2013; Padgett et al., 2012). However, the subcellular mechanism underlying the decrease in $GABA_BR$-activated GIRK currents in VTA DA neurons is not well understood. In rats sensitized to psychostimulants, mRNA for SNX27b (Mrt1b) increases (Kajii et al., 2003), raising the possibility that some of these effects of psychostimulants may be mediated by SNX27.

Enhanced novelty/sensation seeking is a strong indicator of addiction-like behavior in both rodents and humans (Belin et al., 2010; Jupp and Dalley, 2013). Interestingly, $SNX27_{DA}$ KO mice were significantly more active in a novel environment than the two control lines of mice. Moreover, enhanced reaction to novelty in mutant mice often correlates with an augmentation of cocaine response (Bello et al., 2011; Dietrich et al., 2012), and mice lacking SNX27 in DA neurons exhibit a heightened sensitivity to cocaine. Restoration of $GABA_BR$-activated GIRK currents in DA neurons with ectopic expression of GIRK2a completely normalized the cocaine sensitivity, confirming the important role for $GABA_BR$-activated GIRK currents in VTA DA neurons. Fast GABA-evoked inhibitory currents also control VTA DA neuron firing. Genetic manipulations that reduce the amplitude of fast GABA-evoked IPSCs enhance dopamine release and learning of cue-reward associations (Parker et al., 2011), and repeated cocaine administration also reduces $GABA_AR$ signaling, facilitating LTP induction in VTA DA neurons (Liu et al., 2005). Taken together, these studies underscore the importance of inhibitory control of VTA DA neurons in regulating DA release in the brain reward circuit in response to drugs of abuse.

$GABA_B$ receptors have been implicated in reducing addictive behaviors (Tyacke et al., 2010). $GABA_B$ receptors in DA neurons are selectively activated by GABAergic ventral pallidum projections to VTA (Sugita et al., 1992). Silencing ventral pallidum GABAergic afferents onto the VTA increases the population activity of DA neurons and extra-synaptic dopamine release in nucleus accumbens (Floresco et al., 2003) and could represent a mechanism by which diminished $GABA_BR$-GIRK currents by SNX27 trafficking of GIRK channels affect dopamine-dependent behaviors. Together with increased cortical expression of SNX27 following psychostimulant administration (Kajii et al., 2003) and the established role of GIRK channels in cocaine response (Morgan et al., 2003), these data identify a novel SNX27-dependent mechanism of inhibitory plasticity in DA neurons as a potential therapeutic intervention point for addiction and other psychiatric disorders of dopamine dysregulation.

Materials and Methods

Generation of $SNX27_{DA}$ KO mice

Knockout-first promoter driven line $Snx27^{tm1a(KOMP)Wtsi}$ heterozygous animals were purchased from UC Davis KOMP Repository and crossed to flp deleter line B6.SJL-Tg(ACTFLPe)9205Dym/J (JAX stock #005703) to remove selection cassette and create

conditional allele ($Snx27^{fl/fl}$). The founder line was created in C57BL6, eliminating the need for extensive backcrossing.

$Snx27^{fl/fl}$ animals were crossed to DAT-Cre C57BL6 line (Zhuang et al., 2005), then $Snx27^{fl/+}$-DAT-$Cre^{+/-}$ intercrossed to generate $Snx27^{fl/fl}$-DAT-$Cre^{+/-}$ animals. Experimental animals and littermate controls were generated by crossing $Snx27^{fl/fl}$-DAT-$Cre^{+/-}$ ($SNX27_{DA}$ KO) to $Snx27^{fl/fl}$ (conditional line). DAT-$Cre^{+/-}$ crossed to C57Bl/6J were maintained separately, and only $Cre^{+/-}$ animals (DAT-$Cre^{+/-}$) were included in experiments.

Genotyping

Tail biopsies were collected from animals at weaning (>P21) and PCR genotyping was performed using the following primers:

SNX_loxP_geno_F: 5’-AAAGGGCTGGGCGGTAGTGG-3’

SNX_loxP_geno2_R: 5’-CAGGGCCCAGATCATTCAACACTTC-3’

Flp_geno_F: 5’-ACCATAGGGTTGATGAGATGGCCAA-3’

Flp_geno_R: 5’-ACAGCATGACTTGGCTGACATACGTG-3’

Cre320 F: 5’-GAACC TGATG GACAT GTTCA GG-3’

Cre320 R: 5’-AGTGC GTTCG AACGC TAGAG CCTGT-3’

Cre_myo internal control F: 5’-TTACG TCCAT CGTGG ACAGC-3’

Cre_myo internal control R: 5’-TGGGC TGGGT GTTAG CCTTA-3’

Animal husbandry

Animals were housed under constant temperature and humidity on a 12-hr light-dark cycle (light 6 am–6 pm) with food and water available *ad libitum* (except during behavioral analysis). Mixed genotypes were housed together in groups of 2–5, separated by sex. All procedures were performed in the light cycle using IACUC-approved protocols for animal handling at the Salk Institute.

Electrophysiology

Male and female mice age P30-P50 were euthanized with isoflurane, brains removed and horizontal slices prepared from midbrain (200μm) in ice-cold artificial cerebral spinal fluid containing (in mM): NaCl 119, KCl 2.5, $MgCl_2$ 1.3, $CaCl_2$ 2.5, NaH_2PO_4 1.0, $NaHCO_3$ 26.2 and glucose 11, pH 7.2, bubbled with 95% O_2 and 5% CO_2. Slices were equilibrated for ~45 min at 33° C in ACSF supplemented with (in mM): L-Ascorbic acid 0.4, Na Pyruvate 2, myo-Inositol 3, then transferred to a recording chamber equipped with constant perfusion of ACSF (2 ml/min).

Neurons were visualized on an Olympus scope (BX51WI) equipped with fluorescence and whole-cell patch-clamp recordings were made from neurons in the posterior medial VTA, defined as the region medial to the medial terminal nucleus of the accessory optical tract. DA neurons were identified by presence of I_h current, large capacitance (30–50 pF) and

slow spontaneous firing (1–3 Hz) (Cruz et al., 2004; Labouèbe et al., 2007; Lammel et al., 2008; Padgett et al., 2012). Pitx3-GFP mice expressing GFP in DA neurons (Zhao et al., 2004) and viral expression of GFP/YFP in DAT-$Cre^{+/-}$ cells were used to confirm electrophysiological identification of DA neurons.

The internal solution contained (in mM) potassium gluconate 140, NaCl 4, $MgCl_2$ 2, EGTA 1.1, HEPES 5, Na_2ATP 2, sodium creatine phosphate 5 and Na_3GTP 0.6 (pH 7.3) with KOH. Whole-cell voltage-clamp recordings were used to measure GIRK currents. For agonist-induced currents, changes in holding currents (V_m = −35 mV with junction potential −15.7mV) in response to bath application of a saturating dose of baclofen (300 μM) or quinpirole (30 μM) were measured (at −50 mV every 10 sec). Currents were amplified (Molecular Devices Axopatch 200B), filtered at 1 kHz and digitized at 5 kHz (Molecular Devices Digidata 1320). I_h currents were monitored through a series of hyperpolarizing 200 ms voltage steps to −120 mV. Series resistance (Rs) was monitored throughout the experiment and recordings were excluded from analysis if the Rs varied by more than 20%. Clampex 9.0 software was used for data acquisition and analysis. GIRK currents were confirmed by inhibition with Ba^{2+} (1mM), a selective inhibitor of inward rectifiers. For the GTPγS experiment, GTPγS (0.1 μM) was added to the internal solution in place of Na_3GTP. For recording spontaneous IPSCs, the internal solution contained (in mM): 130 CsCl, 4 NaCl, 2 $MgCl_2$, 1.1 EGTA, 5 HEPES, 2 Na_2ATP, 5 sodium creatine-phosphate, 0.6 Na_3GTP. Currents were filtered at 2kHz and digitized at 10kHz. Following whole-cell access, cells were held at −60mV and spontaneous activity recorded for 5 minutes per cell. At the end of recording for at least one cell per genotype, 50μM bicuculline was added to ensure $GABA_AR$ specificity.

Immunohistochemistry & imaging

Animals were anesthetized with 350mg/kg chloral hydrate i.p. and perfused with 4% paraformaldeyde. Brains were post-fixed and cyroprotected in 30% sucrose in PBS. 30μM frozen coronal sections were stained with antibodies for SNX27 (1:1000; rabbit) (Balana et al., 2011) and TH (1:1000, PelFreeze) followed by fluorophore-conjugated secondary. Sections were mounted and imaged on a confocal microscope.

Stereotaxic Surgery

Mice age P24–26 were anesthetized with ketamine/xylazine 10/100mg/kg i.p. and placed in a stereotaxic apparatus. 0.5–1.0μl adeno-associated virus was injected into VTA (x,y,z: +/−0.5mm, −2.4mm, −4.5mm from bregma). Post-operative analgesia was ibuprofen in drinking water for duration of recovery. Animals were allowed to recover at least 12 days prior to use in electrophysiology or behavior experiments. Virus injection was confirmed by presence of GFP/YFP expression in VTA.

Virus Production

pAAV-EF1a-double floxed-EYFP-WPRE-HGH pA (Addgene plasmid 20296) was made into AAV serotype 5 at $>10^{10}$ GC/ml by Salk Institute Viral Vector Core using standard protocols (referred to as AAV DIO-eYFP). Girk2a-EYFP and Snx27b-ires-GFP were sub-

cloned into this vector in at Nhe1 and Asc1 sites and also generated into AAV serotype 5 virus (referred to as AAV DIO *Girk2a*-eYFP and AAV DIO *Snx27b*-ires-GFP).

Open field test

All behavior experiments were conducted in the light phase from 1100–1500. Animals were brought into the testing room at least 30min prior to the start of behavioral experiments, then placed individually into locomotor activity chambers (Med Associates, St Albans, VT) for 30 min or 1 hr, as indicated. Total distance traveled was recorded in 5 min bins. Zone analysis was conducted to determine time spent in center, defined as area of open field excluding peripheral 5 inches on each side of 16×16" square. For cocaine-induced locomotor activity, 24 hours following open field test (day 0), animals were placed in activity chamber for 30 minutes, then received saline (0.9%) solution i.p. and were immediately returned to activity chamber for 30 minutes for 2 consecutive days (days 1–2). On day 3, animals received 20mg/kg cocaine hydrochloride (Sigma-Aldrich) dissociated in saline (0.9%) solution i.p. and were immediately placed in activity chambers for 30 minutes. For virus-injected animals, animals underwent behavioral testing 14–20 days post virus injection. For behavioral experiments, 24–72 hours after the last cocaine injection, brain sections were taken for confirmation of virus expression in VTA.

Statistical analysis

Data were analyzed using Prism 5.0 software. One- or two-way ANOVA with Bonferroni post hoc test or Student's t-test were used as indicated. Significance was defined as $p<0.05$.

Supplementary Material

Refer to Web version on PubMed Central for supplementary material.

Acknowledgments

We thank Karl Deisseroth and Addgene for double-floxed inverted (DIO) backbone constructs, Rene Hen for use of DAT-Cre mice, Salk Institute Viral Vector Core for generating AAV virus, Lawrence Fourgeaud for help with confocal microscopy, Kevin Wickman and laboratory for comments on a previous version of the manuscript, Christian Lüscher for discussions, and Steve Heinemann for use of locomotor activity monitors. We thank members of the Slesinger lab, particularly Seung Lee and Natalie Taylor, for technical help and suggestions to improve these studies. This work was supported by grants from National Institute on Drug Abuse (Ruth L. Kirschstein National Research Service Award F31 DA029401 to M.B.M), Salk Institute Chapman Foundation (M.B.M.), National Institute on Alcohol Abuse and Alcoholism (AA018734 to P.A.S.) and the National Institute on Drug Abuse (DA025236 & DA029706 to P.A.S.).

References

Arora D, Hearing M, Haluk DM, Mirkovic K, Fajardo-Serrano A, Wessendorf MW, Watanabe M, Lujan R, Wickman K. Acute cocaine exposure weakens GABA(B) receptor-dependent G-protein-gated inwardly rectifying K+ signaling in dopamine neurons of the ventral tegmental area. J Neurosci. 2011; 31:12251–12257. [PubMed: 21865468]

Balana B, Bahima L, Bodhinathan K, Taura JJ, Taylor NM, Nettleton MY, Ciruela F, Slesinger PA. Ras-association domain of sorting Nexin 27 is critical for regulating expression of GIRK potassium channels. PLoS One. 2013; 8:e59800. [PubMed: 23536889]

Balana B, Maslennikov I, Kwiatkowski W, Stern KM, Bahima L, Choe S, Slesinger PA. Mechanism underlying selective regulation of G protein-gated inwardly rectifying potassium channels by the

psychostimulant-sensitive sorting nexin 27. Proceedings of the National Academy of Sciences. 2011; 108:5831–5836.

Belin D, Berson N, Balado E, Piazza PV, Deroche-Gamonet V. High-Novelty-Preference Rats are Predisposed to Compulsive Cocaine Self-administration. Neuropsychopharmacology. 2010; 36:569–579. [PubMed: 20980989]

Bello EP, Mateo Y, Gelman DM, Noaín D, Shin JH, Low MJ, Alvarez VA, Lovinger DM, Rubinstein M. Cocaine supersensitivity and enhanced motivation for reward in mice lacking dopamine D2 autoreceptors. Nature Neuroscience. 2011; 14:1033–1038.

Bocklisch C, Pascoli V, Wong JC, House DR, Yvon C, de Roo M, Tan KR, Luscher C. Cocaine disinhibits dopamine neurons by potentiation of GABA transmission in the ventral tegmental area. Science. 2013; 341:1521–1525. [PubMed: 24072923]

Boyer SB, Clancy SM, Terunuma M, Revilla-Sanchez R, Thomas SM, Moss SJ, Slesinger PA. Direct Interaction of GABAB Receptors with M2 Muscarinic Receptors Enhances Muscarinic Signaling. J Neurosci. 2009; 29:15796–15809. [PubMed: 20016095]

Cai L, Loo LS, Atlashkin V, Hanson BJ, Hong W. Deficiency of sorting nexin 27 (SNX27) leads to growth retardation and elevated levels of N-methyl-D-aspartate receptor 2C (NR2C). Mol Cell Biol. 2011; 31:1734–1747. [PubMed: 21300787]

Chang W, Tu C, Cheng Z, Rodriguez L, Chen TH, Gassmann M, Bettler B, Margeta M, Jan LY, Shoback D. Complex formation with the Type B gamma-aminobutyric acid receptor affects the expression and signal transduction of the extracellular calcium-sensing receptor. Studies with HEK-293 cells and neurons. J Biol Chem. 2007; 282:25030–25040. [PubMed: 17591780]

Chung HJ, Qian X, Ehlers M, Jan YN, Jan LY. Neuronal activity regulates phosphorylation-dependent surface delivery of G protein-activated inwardly rectifying potassium channels. Proc Natl Acad Sci U S A. 2009; 106:629–634. [PubMed: 19118198]

Ciruela F, Fernandez-Duenas V, Sahlholm K, Fernandez-Alacid L, Nicolau JC, Watanabe M, Lujan R. Evidence for oligomerization between GABAB receptors and GIRK channels containing the GIRK1 and GIRK3 subunits. Eur J Neurosci. 2010; 32:1265–1277. [PubMed: 20846323]

Cruz HG, Ivanova T, Lunn M-L, Stoffel M, Slesinger PA, Lüscher C. Bidirectional effects of GABAB receptor agonists on the mesolimbic dopamine system. Nature Neuroscience. 2004; 7:153–159.

Cullen PJ, Korswagen HC. Sorting nexins provide diversity for retromer-dependent trafficking events. Nature Cell Biology. 2011; 14:29–37.

Dietrich MO, Bober J, Ferreira JG, Tellez LA, Mineur YS, Souza DO, Gao X-B, Picciotto MR, Araújo I, Liu Z-W, Horvath TL. AgRP neurons regulate development of dopamine neuronal plasticity and nonfood-associated behaviors. Nature Neuroscience. 2012; 15:1108–1110.

Floresco SB, West AR, Ash B, Moore H, Grace AA. Afferent modulation of dopamine neuron firing differentially regulates tonic and phasic dopamine transmission. Nature Neuroscience. 2003; 6:968–973.

Fowler CE, Aryal P, Suen KF, Slesinger PA. Evidence for association of GABA(B) receptors with Kir3 channels and regulators of G protein signalling (RGS4) proteins. J Physiol. 2007; 580:51–65. [PubMed: 17185339]

Frankowska M, Nowak E, Filip M. Effects of GABAB receptor agonists on cocaine hyperlocomotor and sensitizing effects in rats. Pharmacol Rep. 2009; 61:1042–1049. [PubMed: 20081239]

Gainetdinov RR, Premont RT, Bohn LM, Lefkowitz RJ, Caron MG. Desensitization of G protein-coupled receptors and neuronal functions. Annu Rev Neurosci. 2004; 27:107–144. [PubMed: 15217328]

Ghai R, Mobli M, Norwood SJ, Bugarcic A, Teasdale RD, King GF, Collins BM. Phox homology band 4.1/ezrin/radixin/moesin-like proteins function as molecular scaffolds that interact with cargo receptors and Ras GTPases. Proc Natl Acad Sci U S A. 2011; 108:7763–7768. [PubMed: 21512128]

Hayashi H, Naoi S, Nakagawa T, Nishikawa T, Fukuda H, Imajoh-Ohmi S, Kondo A, Kubo K, Yabuki T, Hattori A, Hirouchi M, Sugiyama Y. Sorting Nexin 27 Interacts with Multidrug Resistance-associated Protein 4 (MRP4) and Mediates Internalization of MRP4. Journal of Biological Chemistry. 2012; 287:15054–15065. [PubMed: 22411990]

Hearing M, Kotecki L, Marron Fernandez de Velasco E, Fajardo-Serrano A, Chung HJ, Lujan R, Wickman K. Repeated cocaine weakens GABA(B)-Girk signaling in layer 5/6 pyramidal neurons in the prelimbic cortex. Neuron. 2013; 80:159–170. [PubMed: 24094109]

Inanobe A, Yoshimoto Y, Horio Y, Morishige K-I, Hibino H, Matsumoto S, Tokunaga Y, Maeda T, Hata Y, Takai Y, Kurachi Y. Characterization of G-protein-gated K^+ channels composed of Kir3.2 subunits in dopaminergic neurons of the substantia nigra. J Neurosci. 1999; 19:1006–1017. [PubMed: 9920664]

Jhou TC, Fields HL, Baxter MG, Saper CB, Holland PC. The Rostromedial Tegmental Nucleus (RMTg), a GABAergic Afferent to Midbrain Dopamine Neurons, Encodes Aversive Stimuli and Inhibits Motor Responses. Neuron. 2009; 61:786–800. [PubMed: 19285474]

Johnson SW, North RA. Two types of neurone in the rat ventral tegmental area and their synaptic inputs. J Physiol. 1992; 450:455–468. [PubMed: 1331427]

Joubert L, Hanson B, Barthet G, Sebben M, Claeysen S, Hong W, Marin P, Dumuis A, Bockaert J. New sorting nexin (SNX27) and NHERF specifically interact with the 5-HT4a receptor splice variant: roles in receptor targeting. J Cell Sci. 2004; 117:5367–5379. [PubMed: 15466885]

Jupp B, Dalley JW. Behavioral endophenotypes of drug addiction: Etiological insights from neuroimaging studies. Neuropharmacology. 2013

Kajii Y, Muraoka S, Hiraoka S, Fujiyama K, Umino A, Nishikawa T. A developmentally regulated and psychostimulant-inducible novel rat gene mrt1 encoding PDZ-PX proteins isolated in the neocortex. Molecular Psychiatry. 2003; 8:434–444. [PubMed: 12740601]

Kalivas PW, Stewart J. Dopamine transmission in the initiation and expression of drug- and stress-induced sensitization of motor activity. Brain Res Brain Res Rev. 1991; 16:223–244. [PubMed: 1665095]

Kim E, Sheng M. PDZ domain proteins of synapses. Nat Rev Neurosci. 2004; 5:771–781. [PubMed: 15378037]

Kim Y, Kim S, Lee S, Kim SH, Park ZY, Song WK, Chang S. Interaction of SPIN90 with dynamin I and its participation in synaptic vesicle endocytosis. J Neurosci. 2005; 25:9515–9523. [PubMed: 16221862]

Klitenick MA, DeWitte P, Kalivas PW. Regulation of somatodendritic dopamine release in the ventral tegmental area by opioids and GABA: an in vivo microdialysis study. J Neurosci. 1992; 12:2623–2632. [PubMed: 1319478]

Labouèbe G, Lomazzi M, Cruz HG, Creton C, Luján R, Li M, Yanagawa Y, Obata K, Watanabe M, Wickman K, Boyer SB, Slesinger PA, Lüscher C. RGS2 modulates coupling between GABAB receptors and GIRK channels in dopamine neurons of the ventral tegmental area. Nature Neuroscience. 2007; 10:1559–1568.

Lammel S, Hetzel A, Häckel O, Jones I, Liss B, Roeper J. Unique Properties of Mesoprefrontal Neurons within a Dual Mesocorticolimbic Dopamine System. Neuron. 2008; 57:760–773. [PubMed: 18341995]

Lauffer BEL, Melero C, Temkin P, Lei C, Hong W, Kortemme T, von Zastrow M. SNX27 mediates PDZ-directed sorting from endosomes to the plasma membrane. The Journal of Cell Biology. 2010; 190:565–574. [PubMed: 20733053]

Liu, Q-s; Pu, L.; Poo, M-m. Repeated cocaine exposure in vivo facilitates LTP induction in midbrain dopamine neurons. Nature. 2005; 437:1027–1031. [PubMed: 16222299]

Logothetis DE, Kurachi Y, Galper J, Neer EJ, Clapham DE. The βγ subunits of GTP-binding proteins activate the muscarinic K^+ channel in heart. Nature. 1987; 325:321–326. [PubMed: 2433589]

Lujan R, Marron Fernandez de Velasco E, Aguado C, Wickman K. New insights into the therapeutic potential of Girk channels. Trends Neurosci. 2013

Lujan R, Maylie J, Adelman JP. New sites of action for GIRK and SK channels. Nat Rev Neurosci. 2009; 10:475–480. [PubMed: 19543219]

Lunn ML, Nassirpour R, Arrabit C, Tan J, McLeod I, Arias CM, Sawchenko PE, Yates JR 3rd, Slesinger PA. A unique sorting nexin regulates trafficking of potassium channels via a PDZ domain interaction. Nat Neurosci. 2007; 10:1249–1259. [PubMed: 17828261]

Luscher B, Hauselmann R, Leitgeb S, Rulicke T, Fritschy JM. Neuronal subtype-specific expression directed by the GABA(A) receptor delta subunit gene promoter/upstream region in transgenic mice and in cultured cells. Brain Res Mol Brain Res. 1997; 51:197–211. [PubMed: 9427522]

Lüscher C, Malenka Robert C. Drug-Evoked Synaptic Plasticity in Addiction: From Molecular Changes to Circuit Remodeling. Neuron. 2011; 69:650–663. [PubMed: 21338877]

Lüscher C, Slesinger PA. Emerging roles for G protein-gated inwardly rectifying potassium (GIRK) channels in health and disease. Nature Reviews Neuroscience. 2010; 11:301–315.

Ma D, Zerangue N, Raab-Graham K, Fried SR, Jan YN, Jan LY. Diverse trafficking patterns due to multiple traffic motifs in G protein-activated inwardly rectifying potassium channels from brain and heart. Neuron. 2002; 33:715–729. [PubMed: 11879649]

Mameli M, Bellone C, Brown MT, Luscher C. Cocaine inverts rules for synaptic plasticity of glutamate transmission in the ventral tegmental area. Nat Neurosci. 2011; 14:414–416. [PubMed: 21336270]

Morgan AD, Carroll ME, Loth AK, Stoffel M, Wickman K. Decreased Cocaine Self-Administration in Kir3 Potassium Channel Subunit Knockout Mice. Neuropsychopharmacology. 2003; 28:932–938. [PubMed: 12637950]

Padgett Claire L, Lalive Arnaud L, Tan Kelly R, Terunuma M, Munoz Michaelanne B, Pangalos Menelas N, Martínez-Hernández J, Watanabe M, Moss Stephen J, Luján R, Lüscher C, Slesinger Paul A. Methamphetamine-Evoked Depression of GABAB Receptor Signaling in GABA Neurons of the VTA. Neuron. 2012; 73:978–989. [PubMed: 22405207]

Parker JG, Wanat MJ, Soden ME, Ahmad K, Zweifel LS, Bamford NS, Palmiter RD. Attenuating GABA(A) receptor signaling in dopamine neurons selectively enhances reward learning and alters risk preference in mice. J Neurosci. 2011; 31:17103–17112. [PubMed: 22114279]

Saal D, Dong Y, Bonci A, Malenka RC. Drugs of abuse and stress trigger a common synaptic adaptation in dopamine neurons. Neuron. 2003; 37:577–582. [PubMed: 12597856]

Schultz W. Multiple Dopamine Functions at Different Time Courses. Annual Review of Neuroscience. 2007; 30:259–288.

Seutin V, Johnson SW, North RA. Effect of dopamine and baclofen on N-methyl-D-aspartate-induced burst firing in rat ventral tegmental neurons. Neuroscience. 1994; 58:201–206. [PubMed: 8159294]

Shin N, Lee S, Ahn N, Kim SA, Ahn SG, YongPark Z, Chang S. Sorting Nexin 9 Interacts with Dynamin 1 and N-WASP and Coordinates Synaptic Vesicle Endocytosis. Journal of Biological Chemistry. 2007; 282:28939–28950. [PubMed: 17681954]

Steinberg F, Gallon M, Winfield M, Thomas EC, Bell AJ, Heesom KJ, Tavare JM, Cullen PJ. A global analysis of SNX27-retromer assembly and cargo specicity reveals a function in glucose and metal ion transport. Nat Cell Biol. 2013; 15:461–471. [PubMed: 23563491]

Sugita S, Johnson SW, North RA. Synaptic inputs to GABAA and GABAB receptors originate from discrete afferent neurons. Neurosci Lett. 1992; 134:207–211. [PubMed: 1350333]

Sumioka A. Auxiliary subunits provide new insights into regulation of AMPA receptor trafficking. J Biochem. 2013; 153:331–337. [PubMed: 23426437]

Temkin P, Lauffer B, Jäger S, Cimermancic P, Krogan NJ, von Zastrow M. SNX27 mediates retromer tubule entry and endosome-to-plasma membrane trafficking of signalling receptors. Nature Cell Biology. 2011; 13:717–723.

Terunuma M, Vargas KJ, Wilkins ME, Ramirez OA, Jaureguiberry-Bravo M, Pangalos MN, Smart TG, Moss SJ, Couve A. Prolonged activation of NMDA receptors promotes dephosphorylation and alters postendocytic sorting of GABAB receptors. Proc Natl Acad Sci U S A. 2010; 107:13918–13923. [PubMed: 20643948]

Tsai HC, Zhang F, Adamantidis A, Stuber GD, Bonci A, de Lecea L, Deisseroth K. Phasic Firing in Dopaminergic Neurons Is Sufficient for Behavioral Conditioning. Science. 2009; 324:1080–1084. [PubMed: 19389999]

Tyacke RJ, Lingford-Hughes A, Reed LJ, Nutt DJ. GABAB receptors in addiction and its treatment. Adv Pharmacol. 2010; 58:373–396. [PubMed: 20655489]

Tye KM, Mirzabekov JJ, Warden MR, Ferenczi EA, Tsai H-C, Finkelstein J, Kim S-Y, Adhikari A, Thompson KR, Andalman AS, Gunaydin LA, Witten IB, Deisseroth K. Dopamine neurons

modulate neural encoding and expression of depression-related behaviour. Nature. 2012; 493:537–541. [PubMed: 23235822]

Ungless MA, Whistler JL, Malenka RC, Bonci A. Single cocaine exposure in vivo induces long-term potentiation in dopamine neurons. Nature. 2001; 411:583–587. [PubMed: 11385572]

Valdes JL, Tang J, McDermott MI, Kuo JC, Zimmerman SP, Wincovitch SM, Waterman CM, Milgram SL, Playford MP. Sorting nexin 27 protein regulates trafficking of a p21-activated kinase (PAK) interacting exchange factor (beta-Pix)-G protein-coupled receptor kinase interacting protein (GIT) complex via a PDZ domain interaction. J Biol Chem. 2011; 286:39403–39416. [PubMed: 21926430]

Vanderschuren LJ, Kalivas PW. Alterations in dopaminergic and glutamatergic transmission in the induction and expression of behavioral sensitization: a critical review of preclinical studies. Psychopharmacology (Berl). 2000; 151:99–120. [PubMed: 10972458]

Wang X, Zhao Y, Zhang X, Badie H, Zhou Y, Mu Y, Loo LS, Cai L, Thompson RC, Yang B, Chen Y, Johnson PF, Wu C, Bu G, Mobley WC, Zhang D, Gage FH, Ranscht B, Zhang YW, Lipton SA, Hong W, Xu H. Loss of sorting nexin 27 contributes to excitatory synaptic dysfunction by modulating glutamate receptor recycling in Down's syndrome. Nat Med. 2013; 19:473–480. [PubMed: 23524343]

Zhou H, Chisari M, Raehal KM, Kaltenbronn KM, Bohn LM, Mennerick SJ, Blumer KJ. GIRK channel modulation by assembly with allosterically regulated RGS proteins. Proc Natl Acad Sci U S A. 2012; 109:19977–19982. [PubMed: 23169654]

Zhuang X, Masson J, Gingrich JA, Rayport S, Hen R. Targeted gene expression in dopamine and serotonin neurons of the mouse brain. Journal of Neuroscience Methods. 2005; 143:27–32. [PubMed: 15763133]

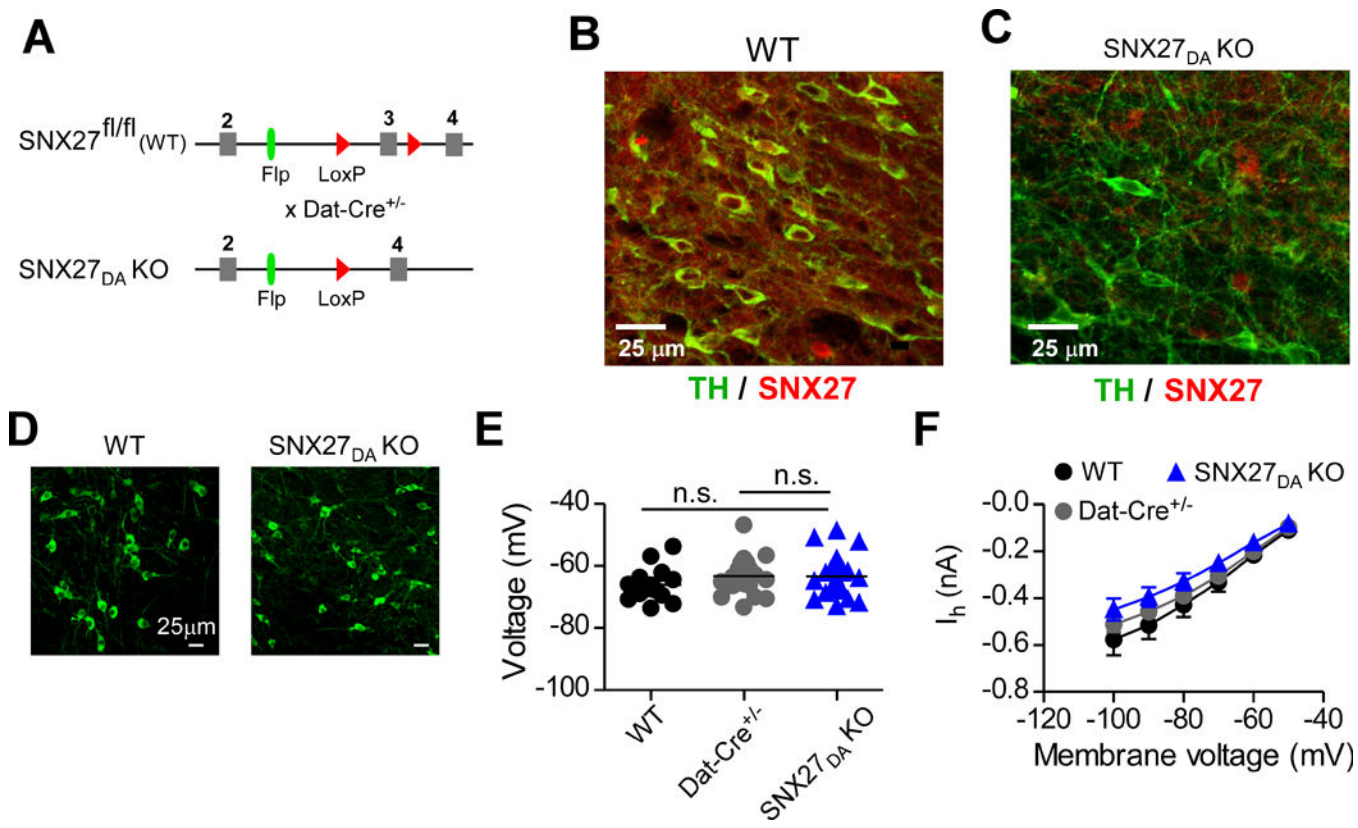

Figure 1. Viability of mice with targeted disruption of SNX27 expression in VTA DA neurons

(**A**) Schematic shows conditional deletion of exon 3 in *Snx27* occurs in DAT-expressing cells. Floxed animals with *SNX27* exon 3 flanked by *loxP* sites were crossed to DAT-Cre$^{+/-}$ line. *SNX27* exon 3 is excised by Cre in DAT-expressing dopamine neurons, referred to as SNX27$_{DA}$ KO mice. (**B,C**) Dual immunofluorescence for SNX27 (red) and TH (green) in coronal sections from WT and SNX27$_{DA}$ KO. **(D)** Immunofluorescence for TH in coronal sections from WT and SNX27$_{DA}$ KO. No apparent difference in TH+ density (7.5± 0.99 for WT, n=2 and 6.0 ± 0.26 for KO, n=2 per 150μm^2. (**E**) Resting membrane potentials were indistinguishable in DA neurons from WT, DAT-Cre$^{+/-}$ and SNX27$_{DA}$ KO mice. (**F**) I_h currents were indistinguishable in DA neurons from WT, Dat-Cre$^{+/-}$ and SNX27$_{DA}$ KO mice.

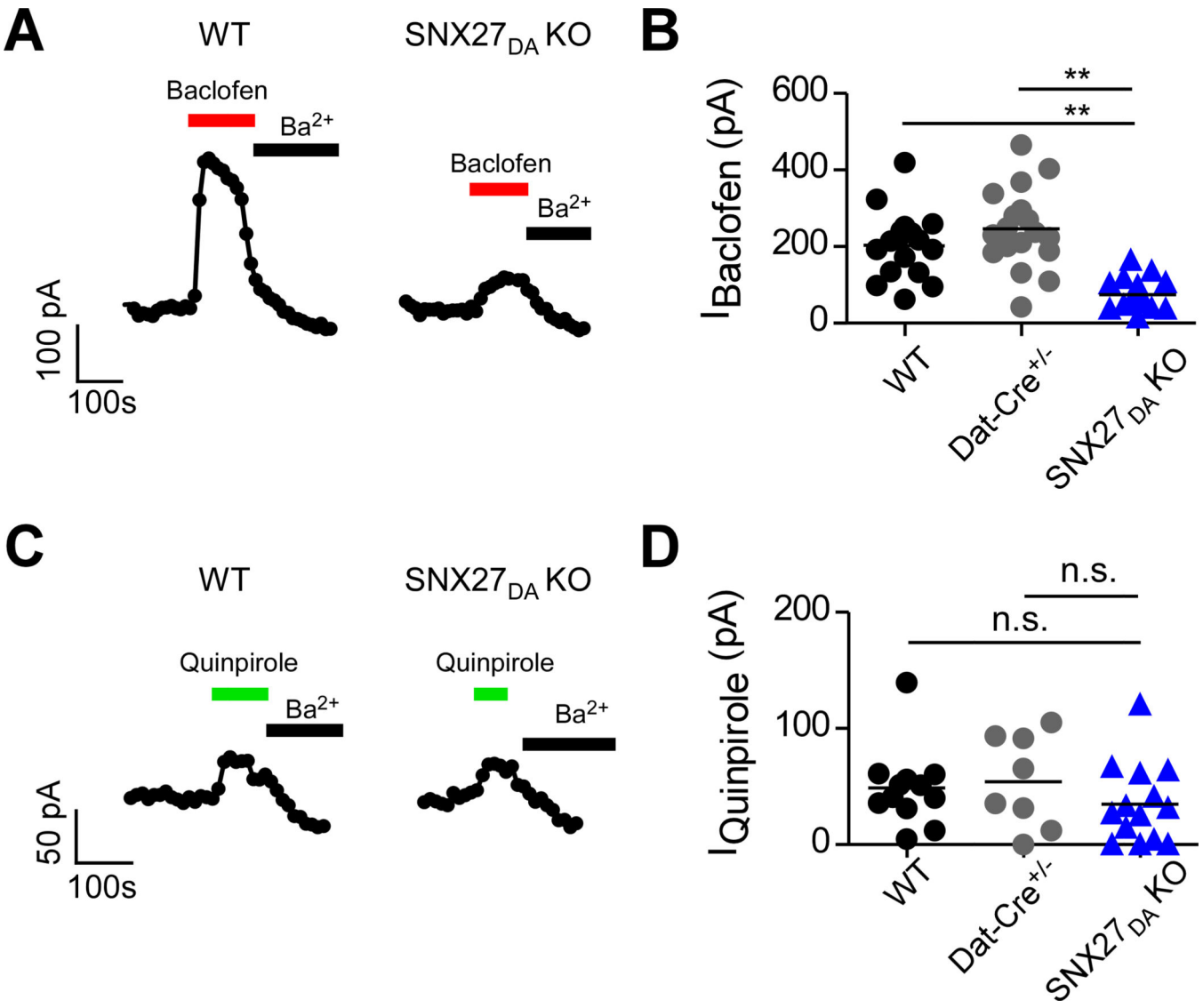

Figure 2. Reduced $GABA_BR$-GIRK currents in VTA DA neurons lacking SNX27 protein

(**A,C**) Whole-cell recordings from VTA DA neurons show baclofen-activated GIRK currents ($I_{Baclofen}$; 300 μM) from WT and $SNX27_{DA}$ KO mice. Extracellular Ba^{2+} (1 mM), a selective inhibitor of inwardly rectifying potassium channels (K_{ir}), decreases I_{Ba}clofen. Outward current measured at −50 mV is plotted as a function of time. (**B,D**) Scatter plot of I_{Ba}clofen for indicated DA neurons. **p<0.01, one-way ANOVA with Bonferroni post hoc test.

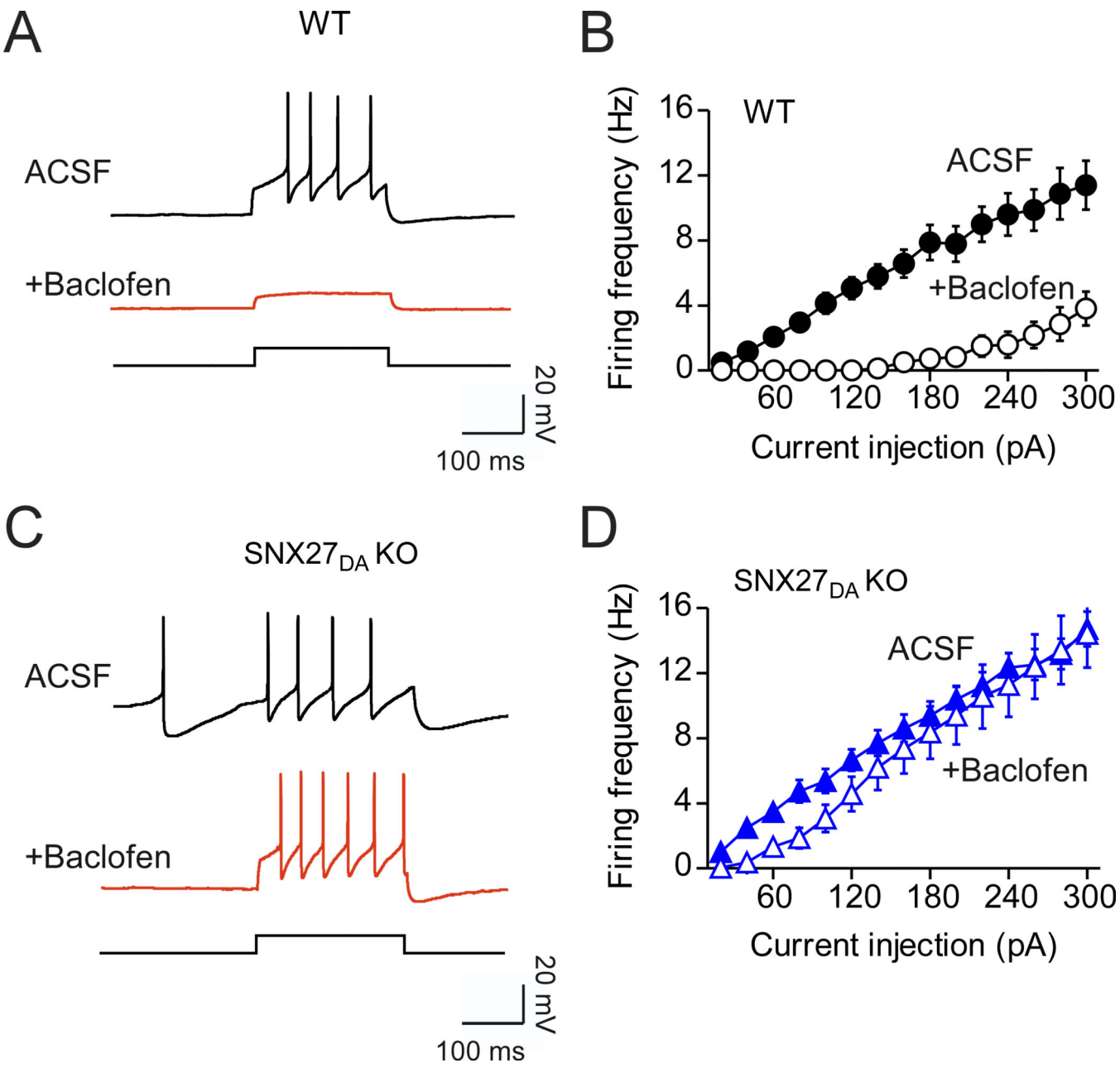

Figure 3. Loss of $GABA_BR$-dependent inhibition of firing in DA neurons of $SNX27_{DA}$ KO mice

(**A**) Current clamp recording shows action potentials in a wild-type DA neuron (200pA injection) before (ACSF) and after application of 300μM baclofen (+Baclofen, red trace). (**B**) Input-output plot shows firing frequency increases with larger current injections (solid circles, ACSF; n=16) and suppression with baclofen (open circles) ($p<0.01$ at 100–300pA, 2-way ANOVA with Bonferroni post hoc test). (**C**) Current clamp recording from DA neuron (200pA injection) before (ACSF) and after application of 300μM baclofen (+Baclofen, red trace). (**D**) Firing frequency is plotted as a function of current injection before (solid triangles, ACSF; n=24) and after baclofen (open triangles). Input-output plot

shows loss of baclofen-dependent inhibition of firing at all current injection levels (n.s. all steps, 2-way ANOVA).

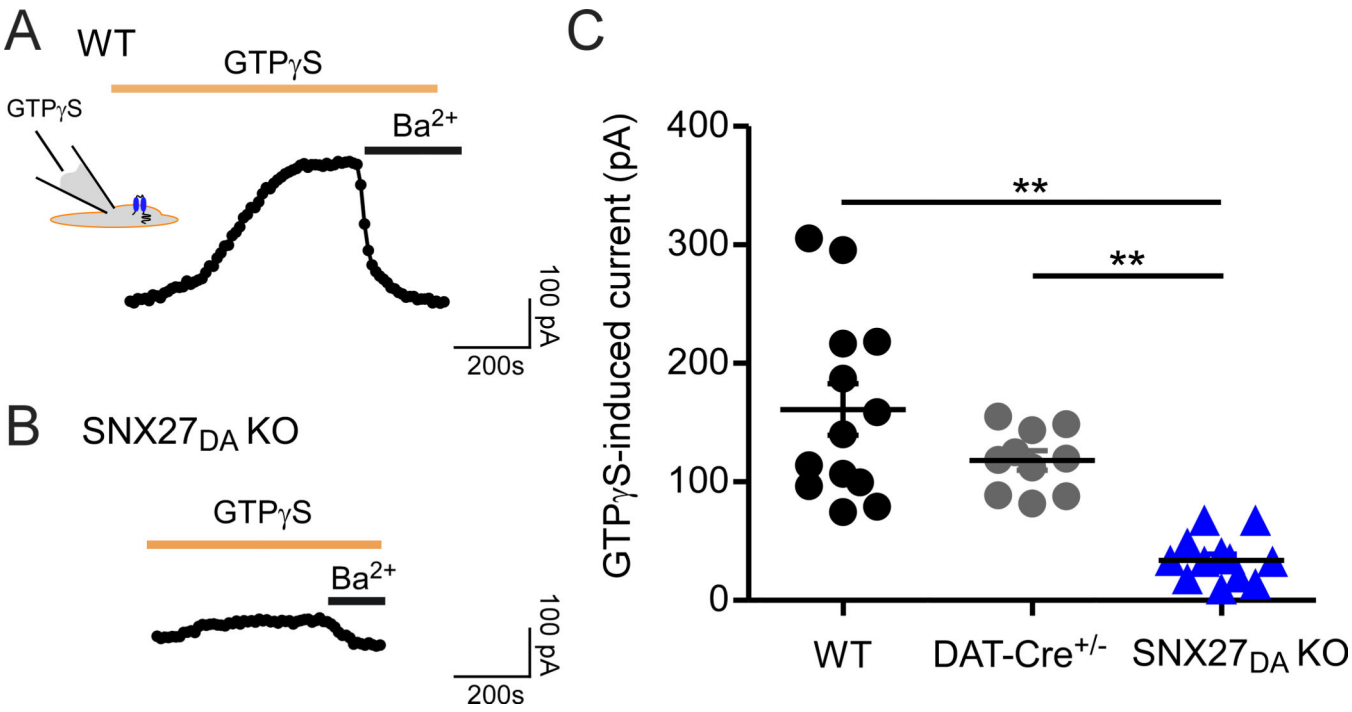

Figure 4. Attenuation of direct G protein-activation of GIRK channels in VTA DA neurons of $SNX27_{DA}$ KO mice

(**A,B**) Outward currents recorded with 100μM GTPγS in the recording pipet from WT or $SNX27_{DA}$ KO DA neuron. A time-dependent increase in outward current occurs with GTPγS, which is inhibited by extracellular Ba^{2+}, consistent with direct activation of GIRK channels (Logothetis et al., 1987). (**C**) Scatter plot shows Ba^{2+}-sensitive activated currents. GTPγS-induced current is significantly reduced in $SNX27_{DA}$ KO neurons (**p<0.01, one-way ANOVA with Bonferroni post hoc test).

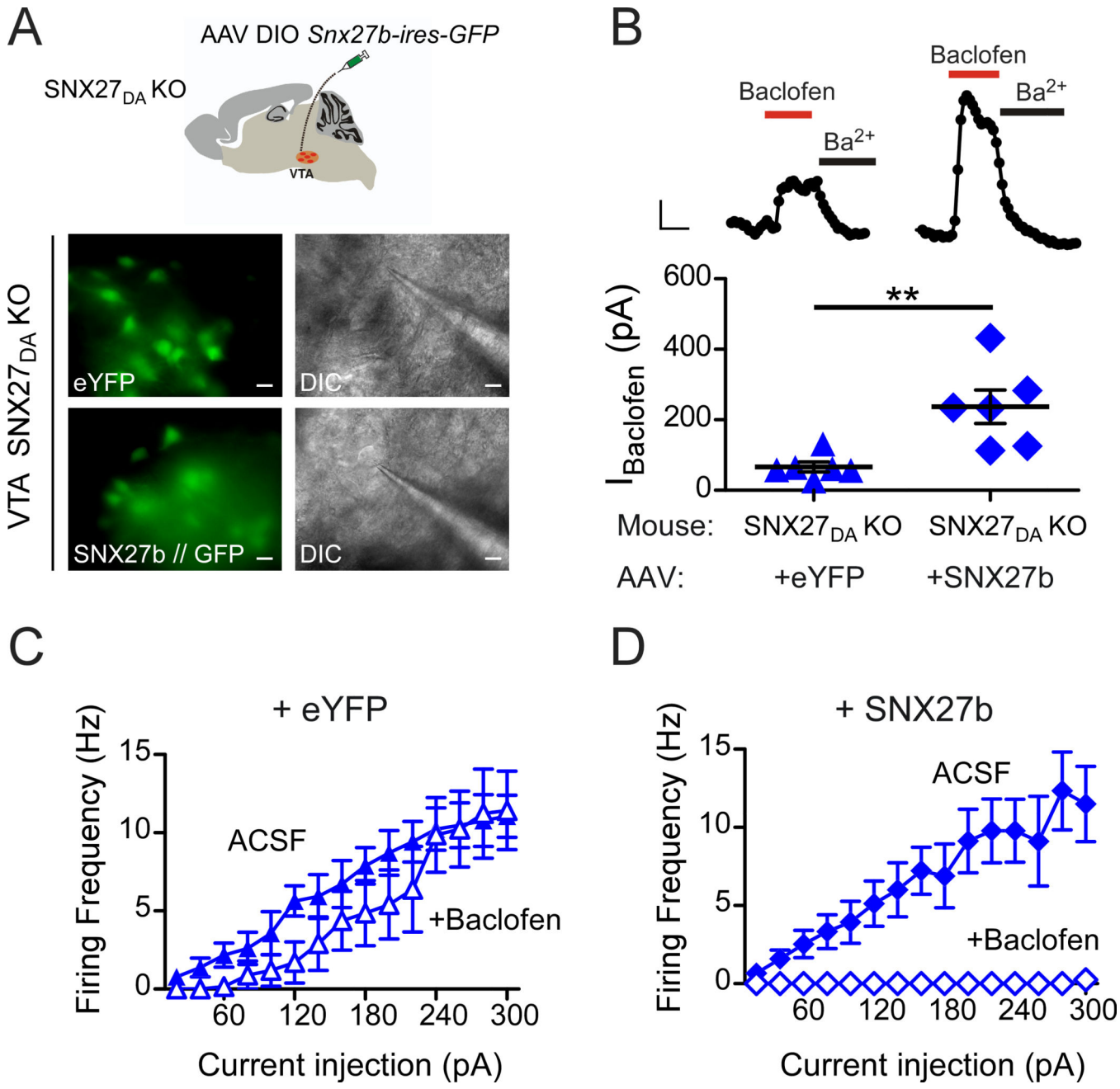

Figure 5. $GABA_B$R-GIRK currents and inhibition are restored with expression of SNX27b in VTA DA neurons of $SNX27_{DA}$ KO mice

(**A**) Schematic shows stereotaxic injection of AAV DIO-*Snx27b*-ires-GFP into VTA of $SNX27_{DA}$ KO mice. Fluorescence and DIC images of eYFP/GFP+ cell selected for recording from *ex vivo* midbrain section of $SNX27_{DA}$ KO with either AAV DIO-eYFP or AAV DIO-Snx27b-ires-GFP (scale bar: 20 μm). (**B**) Top, whole-cell recordings from VTA DA neurons show baclofen-activated GIRK currents ($I_{Baclofen}$; 300 μM) from WT and $SNX27_{DA}$ KO mice injected with AAV DIO-eYFP or AAV DIO-Snx27b-ires-GFP, and inhibition with Ba^{2+} (1 mM). Scale bar; 100 s and 50 pA. Bottom, baclofen-induced currents of Snx27b-ires-GFP positive cells are significantly larger compared to +eYFP (**p<0.01,

Student's t test). Scatter plot of $I_{Baclofen}$ for indicated DA neurons with average current indicated by solid black bar. (**C,D**) Input-output plots show firing frequency increase with larger current injections in the absence (solid circles, ACSF) and presence (filled circles) of baclofen for DA neurons infected with eYFP (**C**) (n=6) or SNX27-ires-GFP (**D**) (n=6) ($p<0.01$ absence versus presence baclofen, 160–300pA, 2-way ANOVA with Bonferroni post hoc test).

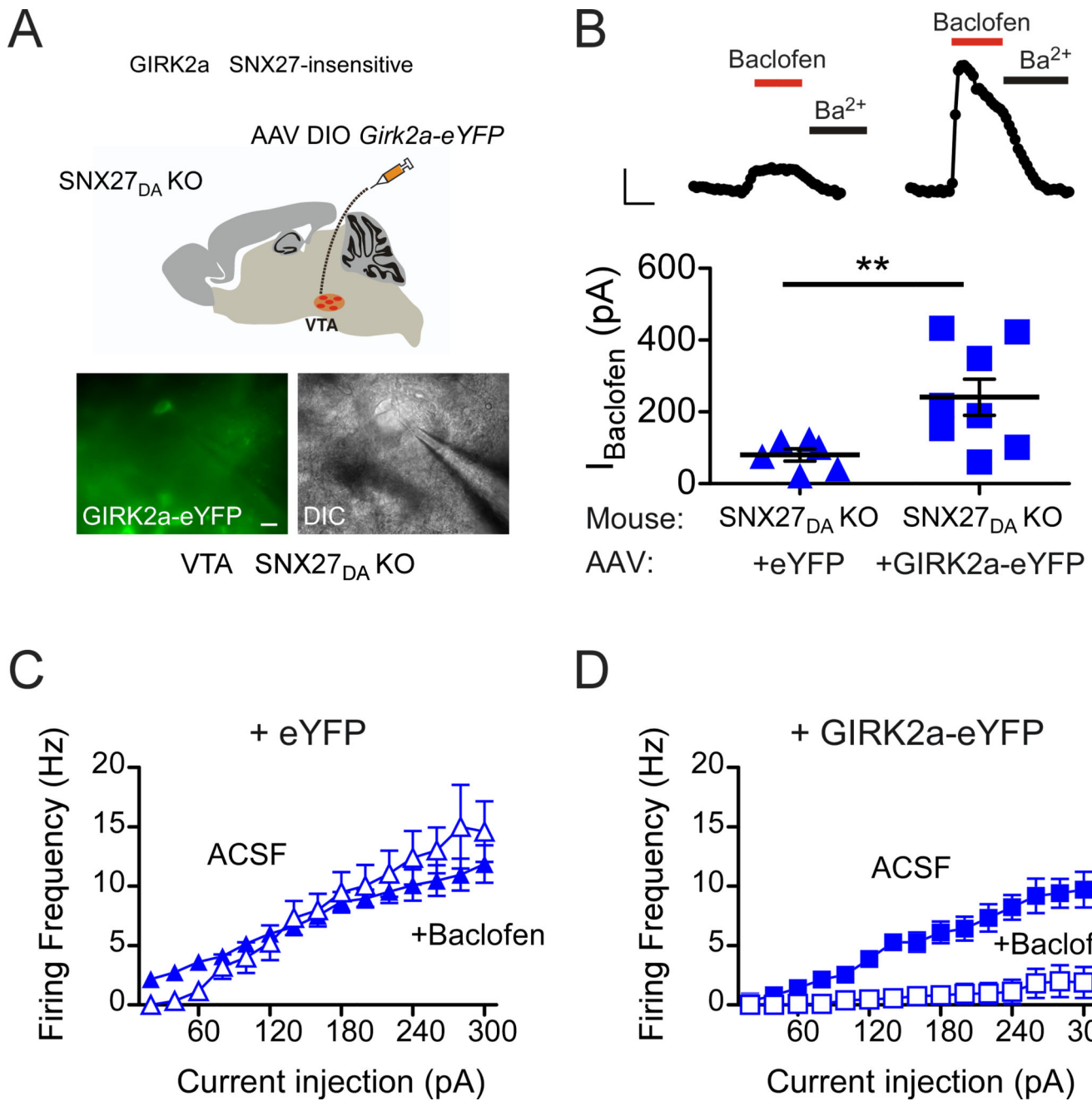

Figure 6. Expression of SNX27-insensitive GIRK2a in VTA DA neurons of $SNX27_{DA}$ KO mice restores $GABA_B$R-activated GIRK currents and inhibition

(**A**) Schematic shows stereotaxic injection of AAV *DIO-GIRK2a-eYFP* into VTA of $SNX27_{DA}$ KO mice. Fluorescence and DIC images of eYFP positive cell selected for recording from *ex vivo* midbrain section of $SNX27_{DA}$ KO mice injected with AAV DIO-Girk2a-eYFP. (scale bar: 20 μm) (**B**) Top, whole-cell recordings from VTA DA neurons show baclofen-activated GIRK currents (I_{Ba}clofen; 300 μM) from WT and $SNX27_{DA}$ KO mice injected with AAV DIO-eYFP or AAV DIO-Girk2a-eYFP, and response to Ba^{2+} (1 mM). Scale bar is 100 s and 100 pA. Bottom, baclofen-induced currents in GIRK2a-eYFP

positive cells are significantly increased from eYFP+ cells (**p<0.05, Student's t test). Scatter plot of I_{Ba}clofen for indicated DA neurons with average current indicated by solid black bar. (**C,D**) Input-output plots show firing frequency increases as a function of larger current injections in the absence (solid circles, ACSF) and presence of baclofen for DA neurons cells infected with eYFP (n=6) (**C**) or GIRK2a-eYFP (n=8) (**D**). Baclofen inhibits firing activity in GIRK2a-eYFP expressing DA neurons (**D**) but not in eYFP expressing neurons (**C**) of $SNX27_{DA}$ KO mice (p<0.01 absence versus presence baclofen at 140–300pA, 2-way ANOVA with Bonferroni post hoc test).

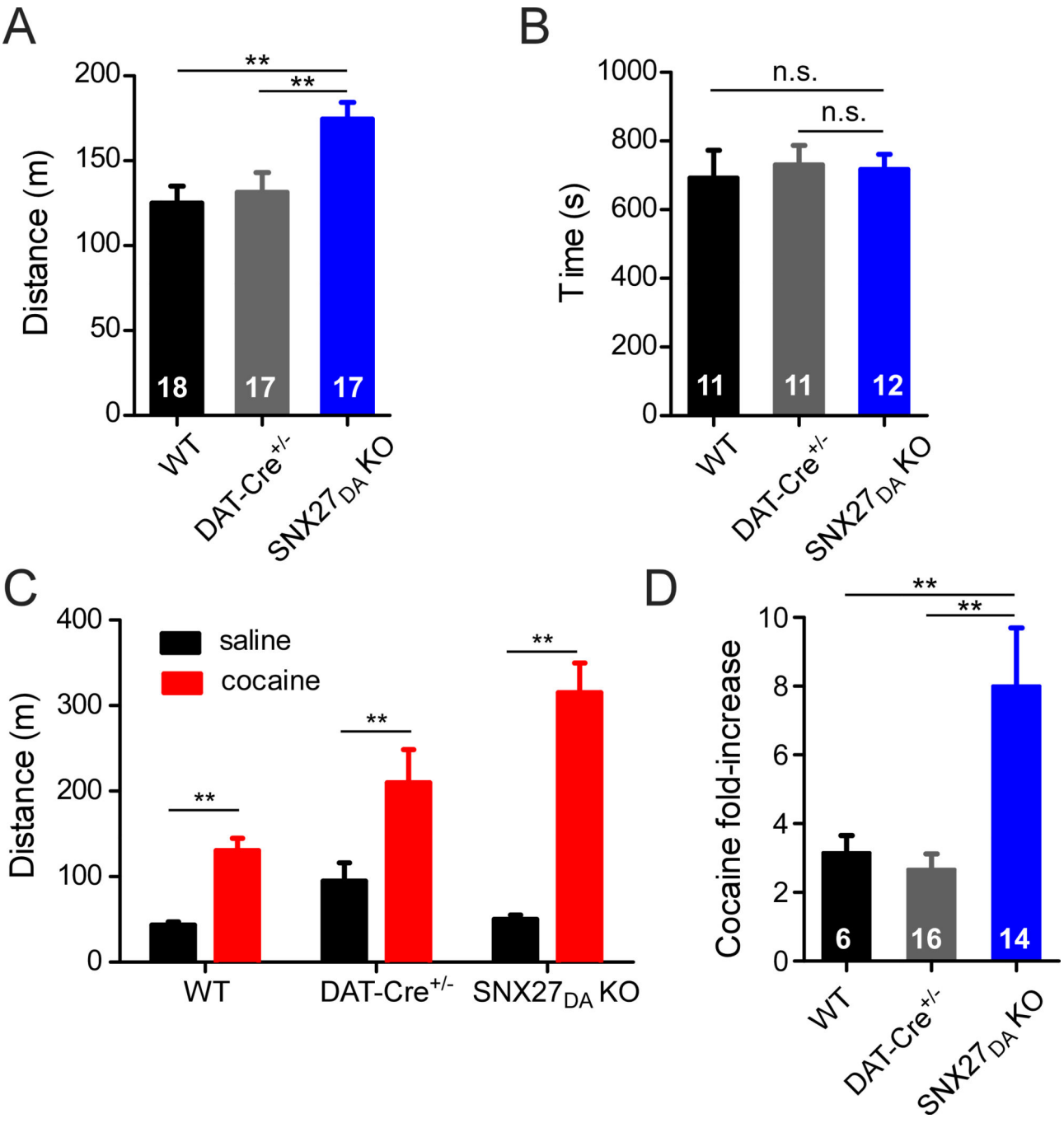

Figure 7. Enhanced cocaine locomotor response in $SNX27_{DA}$ KO mice

(**A**) Total distance traveled in novel open field environment by WT (n=18), DAT-$Cre^{+/-}$ (n=17), and $SNX27_{DA}$ KO (n=17) mice over 1 hour (**p<0.01 vs WT, p<0.05 vs DAT-$Cre^{+/-}$, one-way ANOVA with Bonferroni post hoc test). (**B**) No significant change in thigmotaxis for $SNX27_{DA}$ KO mice (n=12) vs. WT (n=11) or vs. DAT-$Cre^{+/-}$ (n=11). Time spent in center of chamber (central 10” squared of 16” squared chamber, n.s. one-way ANOVA). (**C**) Heightened sensitivity to cocaine in $SNX27_{DA}$ KO mice. Locomotor activity measured in WT (n=6), DAT-$Cre^{+/-}$ (n=16) or $SNX27_{DA}$ KO (n=14) mice following a

single injection (i.p.) of saline (0.9%) or cocaine (20mg/kg). (**p<0.05 cocaine vs. saline, two-way ANOVA with Bonferroni post hoc test). (**D**) Fold increase in locomotor activity with cocaine measured over 30 minute period. (**p<0.05, One-way ANOVA with Bonferroni post hoc test).

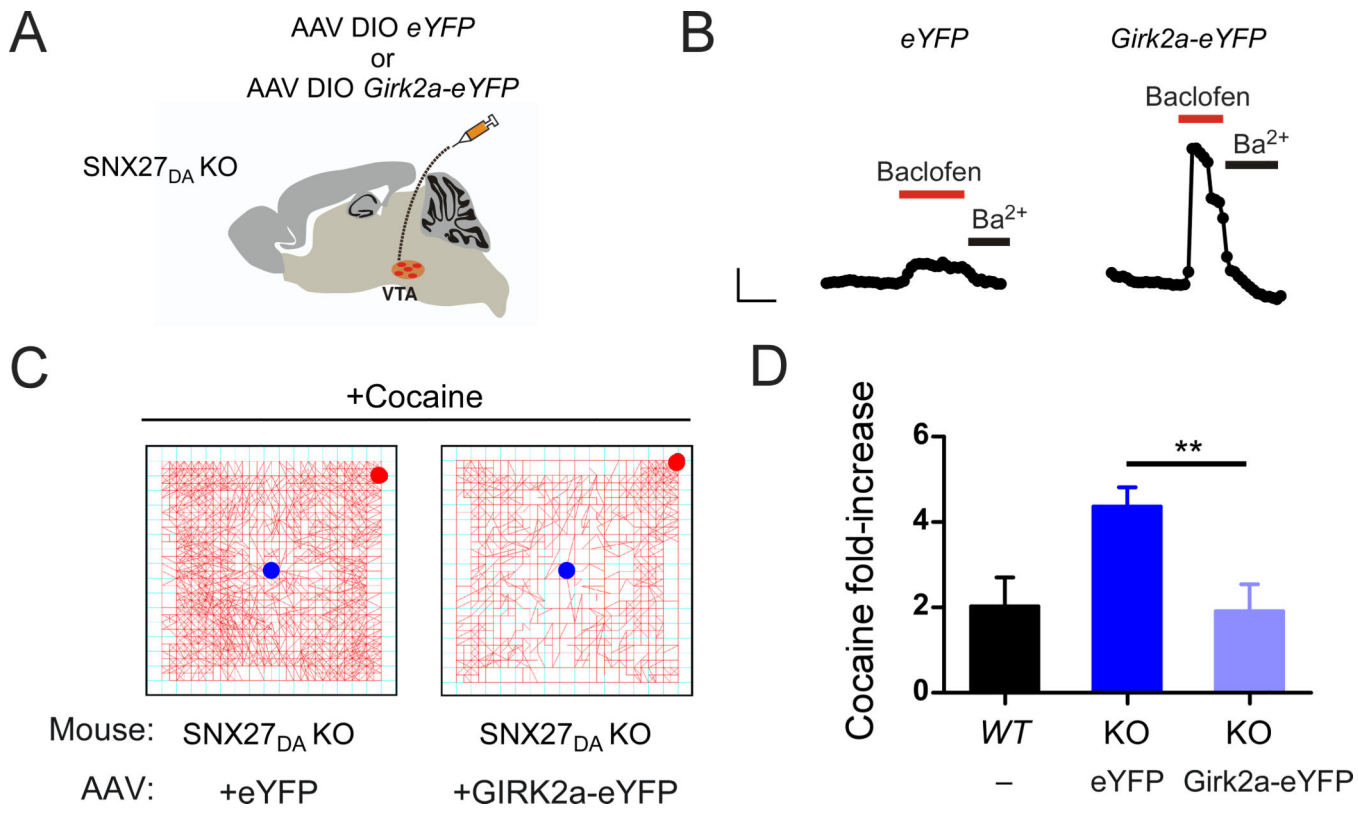

Figure 8. SNX27-insensitive GIRK2a expression in DA neurons of SNX27$_{DA}$ KO mice restores normal response to cocaine

(**A**) Schematic shows stereotaxic injection of AAV DIO *GIRK2a-eYFP* or AAV DIO *eYFP* into VTA of SNX27$_{DA}$ KO mice. (**B**) Whole-cell recordings from VTA DA neurons show rescue of baclofen-activated GIRK currents (I_{Ba}clofen; 300 μM) in SNX27$_{DA}$ KO mice injected with AAV DIO-GIRK2a-eYFP. Scale bar is 100 s and 100 pA. (**C**) Locomotor activity plots show change in activity following a single cocaine injection (20 mg/kg) for a SNX27$_{DA}$ KO mouse expressing eYFP (left) or GIRK2a-eYFP (right). Starting and ending points indicated by blue and red circles, respectively. Note reduced activity in mouse expressing GIRK2a. (**D**) Bar graph shows fold-increase in locomotor activity with cocaine (20 mg/kg) for uninfected WT mice (n=5) and SNX27$_{DA}$ KO mice injected with either AAV DIO eYFP (n=3) or AAV DIO GIRK2a-eYFP (n=3) (**p<0.05 eYFP vs GIRK2a-eYFP, unpaired t-test).